Supporting Information for

# Iron complexes in trigonal tris(alkoxide) ligand environments: synthesis, structures, and oxidation reactivity

Matthew B. Chambers,[a,b] Stanislav Groysman,[a] Dino Villagrán[a] and Daniel G. Nocera[a,b,]*

[a] *Department of Chemistry, 6–335, Massachusetts Institute of Technology, 77 Massachusetts Ave., Cambridge, MA 02139–4307*

[b] *Department of Chemistry and Chemical Biology, Harvard University, 12 Oxford Street, Cambridge, MA 02138–2902*

dnocera@fas.harvard.edu

**Table S1**. Crystal data and structure refinement for **1**, **3**–**9**.

| | **1** | **3** | **4** | **5** | **6** |
|---|---|---|---|---|---|
| formula | $C_{34}H_{71}FeO_4$ | $C_{34}H_{65}FeLiO_4$ | $C_{38}H_{79}FeKO_5$ | $C_{50}H_{103}FeKO_{13}$ | $C_{33}H_{72}FeNO_4$ |
| Fw, g/mol | 599.76 | 600.65 | 710.99 | 1007.27 | 602.77 |
| temperature | 110(2) K | 110(2) K | 110(2) K | 110(2) K | 110(2) K |
| cryst system | triclinic | monoclinic | monoclinic | monoclinic | monoclinic |
| space group | *P*–1 | $P2_1$ | *C*2/c | $P2_1/c$ | $P2_1/n$ |
| color | yellow | green | green | yellow | yellow |
| *Z* | 4 | 2 | 4 | 4 | 4 |
| *a*, Å | 11.526 (1) | 9.146(1) | 18.420(1) | 11.381(3) | 9.932(1) |
| *b*, Å | 17.383(1) | 16.534(1) | 15.878(1) | 17.218(5) | 19.091(2) |
| *c*, Å | 19.912(2) | 12.176(1) | 16.783(1) | 29.190(9) | 18.937(2) |
| $\alpha$, deg | 65.010(1) | 90.00 | 90.00 | 90.0 | 90.00 |
| $\beta$, deg | 84.451(1) | 92.818(1) | 122.454(1) | 91.295(5) | 100.376(2) |
| $\gamma$, deg | 77.465(1) | 90.00 | 90.00 | 90.00 | 90.00 |
| *V*, A$^3$ | 3529.8(4) | 1839.0(2) | 4142.2(4) | 5719(3) | 3532.0(8) |
| $d_{calcd}$, g/cm$^3$ | 1.129 | 1.085 | 1.140 | 1.170 | 1.134 |
| $\mu$, mm$^{-1}$ | 0.460 | 0.441 | 0.501 | 0.392 | 0.460 |
| $2\theta$, deg | 56.78 | 56.54 | 53.740 | 47.94 | 50.00 |
| $R1^a$ (all data) | 0.0710 | 0.0641 | 0.0415 | 0.0644 | 0.0568 |
| $wR2^b$ (all data) | 0.1328 | 0.1204 | 0.0988 | 0.1088 | 0.0904 |
| $R1^b$ [(I>2σ)] | 0.0469 | 0.0461 | 0.0344 | 0.0422 | 0.0377 |
| *wR*2 [(I>2σ)] | 0.1173 | 0.1085 | 0.0927 | 0.958 | 0.0811 |
| GOF ($F^2$) | 1.032 | 1.034 | 1.042 | 1.013 | 1.023 |

[a] $R1 = \Sigma||F_o| - |F_c||/\Sigma|F_o|$. [b] $wR2 = (\Sigma(w(F_o^2 - F_c^2)^2)/\Sigma(w(F_o^2)^2))^{1/2}$. [c] GOF = $(\Sigma w(F_o^2 - F_c^2)^2/(n - p))^{1/2}$ where *n* is the number of data and *p* is the number of parameters refined.

**Table S1** (cont.). Crystal data and structure refinement for **1**, **3**–**9**.

| | **7** | **7a** | **7b** | **8** | **9** |
|---|---|---|---|---|---|
| formula | $C_{52}H_{112}FeLiO_{10}$ | $C_{38}H_{80}FeLiO_6$ | $C_{30}H_{64}FeLiO_4$ | $C_{38}H_{78}FeLiO_6$ | $C_{50}H_{104}FeKO_{14}$ |
| Fw, g/mol | 960.21 | 695.81 | 551.60 | 693.79 | 1024.33 |
| temperature | 110(2) K | 110(2) K | 110(2) K | 110(2) K | 110(2) K |
| cryst system | triclinic | triclinic | triclinic | triclinic | triclinic |
| space group | *P*–1 | *P*–1 | *P*–1 | *P*–1 | *P*–1 |
| color | Yellow | yellow | yellow | yellow | yellow |
| *Z* | 2 | 2 | 2 | 2 | 2 |
| *a*, Å | 11.990(5) | 12.107(1) | 11.145(2) | 12.082(1) | 11.4144(7) |
| *b*, Å | 17.034(5) | 12.546(1) | 11.463(2) | 12.592(1) | 16.199(1) |
| *c*, Å | 17.077(6) | 16.007(1) | 15.124(2) | 15.886(1) | 17.684(1) |
| $\alpha$, deg | 119.693(9) | 87.035(10) | 69.484(2) | 89.912(1) | 99.317(1) |
| $\beta$, deg | 90.078(6) | 70.968(1) | 81.278(3) | 70.403(1) | 90.255(1) |
| $\gamma$, deg | 90.019(5) | 62.728(1) | 63.207(2) | 64.822(1) | 109.732(1) |
| *V*, A$^3$ | 3030(2) | 2029.2(2) | 1615.3(4) | 2032.0(2) | 3031.1(3) |
| $d_{calcd}$, g/cm$^3$ | 1.053 | 1.139 | 1.134 | 1.134 | 1.126 |
| $\mu$, mm$^{-1}$ | 0.296 | 0.411 | 0.496 | 0.411 | 0.392 |
| 2$\theta$, deg | 45.00 | 55.12 | 52.82 | 54.88 | 50.40 |
| *R*1[a] (all data) | 0.1325 | 0.0587 | 0.1245 | 0.0766 | 0.0664 |
| *wR*2[b] (all data) | 0.2876 | 0.0998 | 0.3000 | 0.1947 | 0.1264 |
| *R*1[b] [(I>2σ)] | 0.1042 | 0.0402 | 0.0886 | 0.0660 | 0.0472 |
| *wR*2 [(I>2σ)] | 0.2708 | 0.0905 | 0.2878 | 0.1831 | 0.1143 |
| GOF ($F^2$) | 1.052 | 1.016 | 1.123 | 1.022 | 0.993 |

[a] $R1 = \Sigma||F_o| - |F_c||/\Sigma|F_o|$. [b] $wR2 = (\Sigma(w(F_o^2 - F_c^2)^2)/\Sigma(w(F_o^2)^2))^{1/2}$. [c] GOF = $(\Sigma w(F_o^2 - F_c^2)^2/(n - p))^{1/2}$ where *n* is the number of data and *p* is the number of parameters refined.

**Table S1 (cont)**. Crystal data and structure refinement for $[Fe(ditox)_3(CH_2CN)][K(15C5)_2]$ (**10**).

| | **10** |
|---|---|
| formula | $C_{52}H_{105}O_{13}N_1Fe_1K_1$ |
| Fw, g/mol | 1047.32 |
| temperature | 110(2) K |
| cryst syst | monoclinic |
| space group | $P2_1/n$ |
| color | yellow |
| $Z$ | 4 |
| $a$, Å | 20.214(1) |
| $b$, Å | 15.116(1) |
| $c$, Å | 20.882(1) |
| $\alpha$, deg | 90.00) |
| $\beta$, deg | 113.692(1) |
| $\gamma$, deg | 90.00 |
| $V$, A$^3$ | 5843.4(5) |
| $d_{calcd}$, g/cm$^3$ | 1.190 |
| $\mu$, mm$^{-1}$ | 0.386 |
| $2\theta$, deg | 50.07 |
| $R1^a$ (all data) | 0.0557 |
| $wR2^b$ (all data) | 0.1073 |
| $R1^b$ [(I>2σ)] | 0.0393 |
| $wR2$ [(I>2σ)] | 0.0997 |
| GOF ($F^2$) | 0.987 |

[a] $R1 = \Sigma||F_o| - |F_c||/\Sigma|F_o|$. [b] $wR2 = (\Sigma(w(F_o^2 - F_c^2)^2)/\Sigma(w(F_o^2)^2))^{1/2}$. [c] GOF $= (\Sigma w(F_o^2 - F_c^2)^2/(n - p))^{1/2}$ where $n$ is the number of data and $p$ is the number of parameters refined.

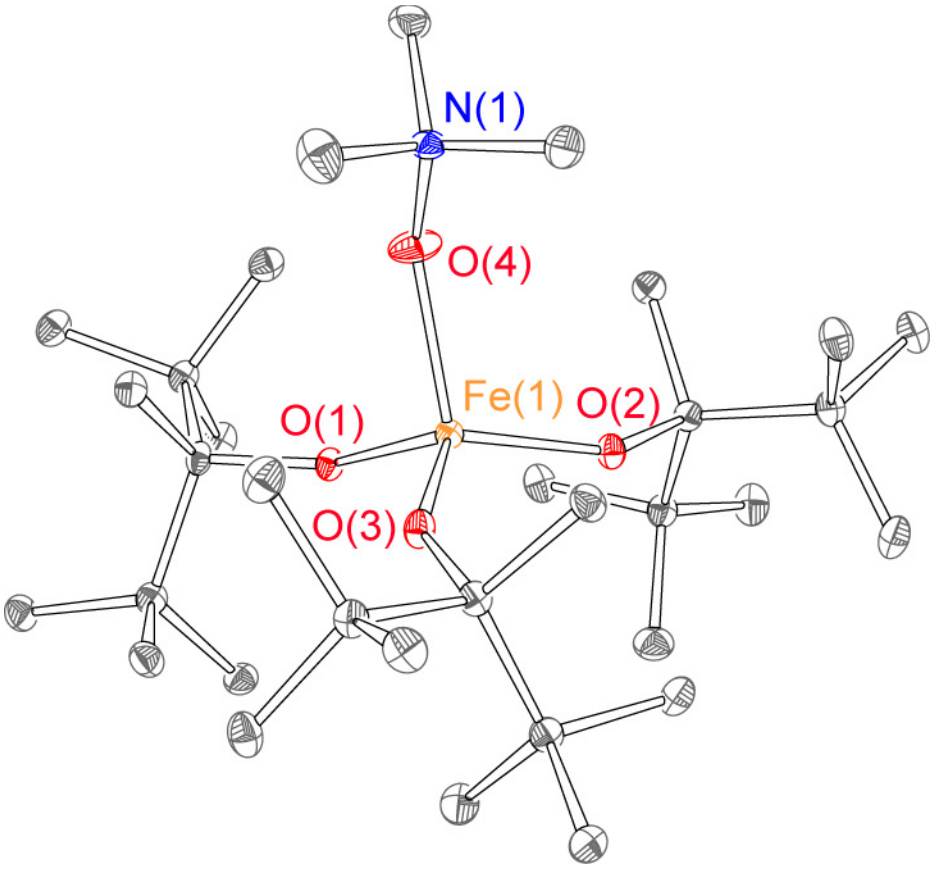


**Figure S1.** Structure of $Fe(ditox)_3(ONMe_3)$ (**6**), 50% probability ellipsoids. Hydrogen atoms omitted for clarity. Selected bond distances: d(Fe1–O1) = 1.840(1) Å, d(Fe1–O2) = 1.843(2) Å, d(Fe1–O3) = 1.838(2) Å, d(Fe1–O4) = 1.979(2) Å, d(O4–N1) = 1.397(2) Å. Selected bond angles: ∠(O1–Fe1–O2) = 113.9(1)°, ∠(O1–Fe1–O3) = 112.2(1)°, ∠(O2–Fe1–O3) = 112.6(1)°, ∠(O1–Fe1–O4) = 107.4(1)°, ∠(O2–Fe1–O4) = 112.9(1)°, ∠(O3–Fe1–O4) = 96.6(1)°, ∠(Fe1–O4–N1) = 137.2(1)°.

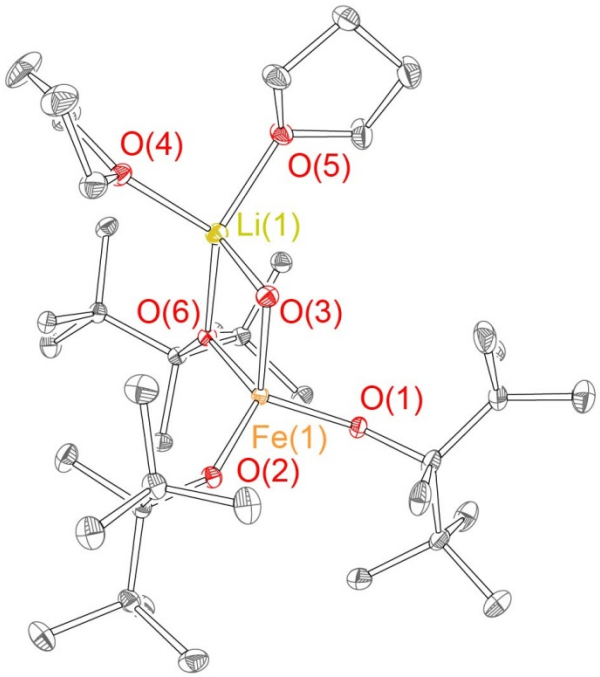


**Figure S2** Structure of $Fe(ditox)_3(OH)Li(THF)_2$, (**7a**), 50% probability ellipsoids. H atoms, co–crystallized solvent molecules, and alternative conformations of $^t$Bu groups are omitted for clarity. Selected bond distances: d(Fe1–O1) = 1.840(1) Å, d(Fe1–O2) = 1.834(1) Å, d(Fe1–O3) = 1.916(2) Å, d(Fe1–O6) = 1.919(1) Å, d(Li1–O4) = 1.875(4) Å, d(Li1–O6) = 2.029(3) Å Selected bond angles: ∠(O1–Fe1–O2) =110.7(1)°, ∠(O1–Fe1–O6) = 110.4(1)°, ∠(O2–Fe1–O6) = 123.7(1)°, ∠(O1–Fe1–O3) = 111.2(1)°, ∠(O2–Fe1–O3) = 111.2(1)°, ∠(O6–Fe1–O3) = 87.4(1)°, ∠(Fe1–O3–Li1) 96.2(2)°.

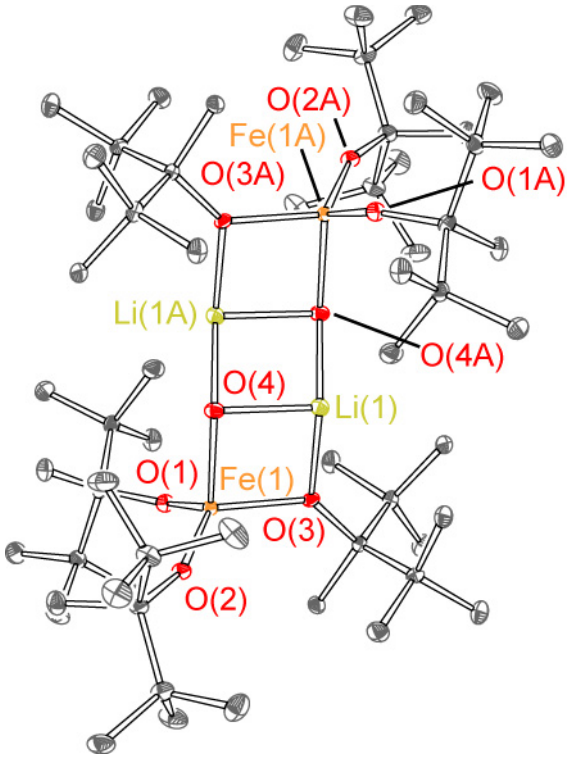


**Figure S3.** Structure [Fe(ditox)(OH)Li]$_2$, (**7b**), 30% probability ellipsoids. H atoms are omitted for clarity. Selected bond distances: d(Fe1–O1) = 1.812(5) Å, d(Fe1–O2) = 1.804(5) Å, d(Fe1–O3) = 1.913(5) Å, d(Fe1–O4) = 1.981(5) Å, d(Li–O3) = 1.880(2) Å, d(Li–O4) = 1.990(2) Å. Selected bond angles: ∠(O1–Fe1–O2) = 121.2(2)°, ∠(O1–Fe1–O3) = 108.8(2)°, ∠(O2–Fe1–O3) = 117.0(2)°, ∠(O1–Fe1–O4) = 110.2(2)°, ∠(O2–Fe1–O4) = 106.6(2)°, ∠(O3–Fe1–O4) = 87.7(2)°, ∠(O3–Li1–O4) = 88.3(5)°.

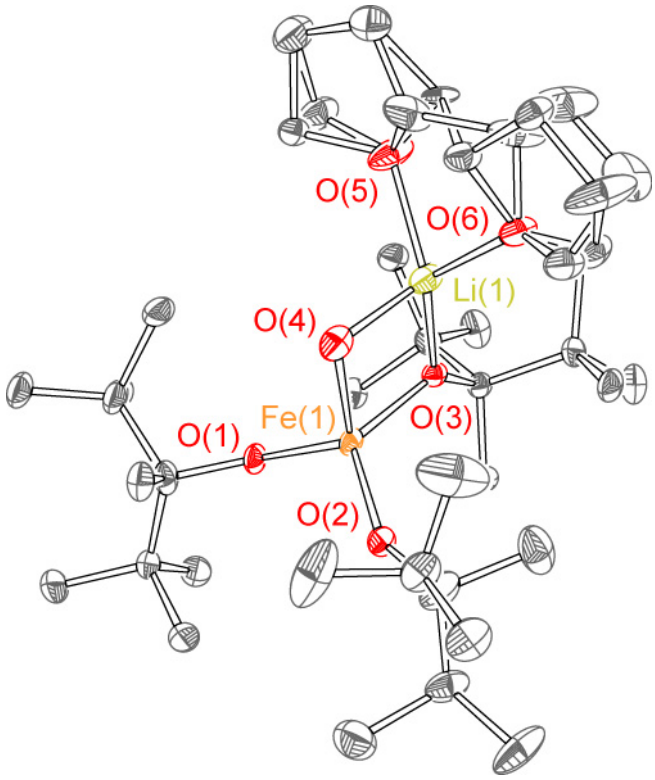


**Figure S4.** Structure of $Fe(ditox)_3(OH)Li(C_8O_2H_{14})$, (**8**), showing both enantiomers of di–THF, 30% probability. H atoms and alternative conformations of $^t$Bu groups are omitted for clarity. Selected bond distance: d(Fe1–O1) = 1.836(2) Å, d(Fe1–O2) = 1.823(2) Å, d(Fe1–O3) = 1.919(2) Å, d(Fe1–O4) = 1.920(2) Å, d(Li1–O3) = 1.949(5) Å, d(Li1–O4) = 1.885(7) Å, d(Li1–O5) = 1.995(5) Å, d(Li1–O6) = 2.014(5) Å. Selected bond angles: ∠(O1–Fe–O2) = 111.4(1)°, ∠(O1–Fe1–O3) = 111.5(1)°, ∠(O2–Fe1–O3) = 121.8(1)°, ∠(O1–Fe1–O4) = 111.4(1)°, ∠(O2–Fe1–O4) = 110.6(1)°, ∠(O3–Fe1–O4) = 87.9(1)°, ∠(O3–Li1–O4) = 88.0(2)°, ∠(O3–Li1–O5) = 135.3(3)°, ∠(O3–Li1–O6) = 129.2(3)°, ∠(O4–Li1–O5) = 109.3(3)°, ∠(O4–Li1–O6) = 111.1(3)°, ∠(O5–Li1–O6) = 83.6(2)°.

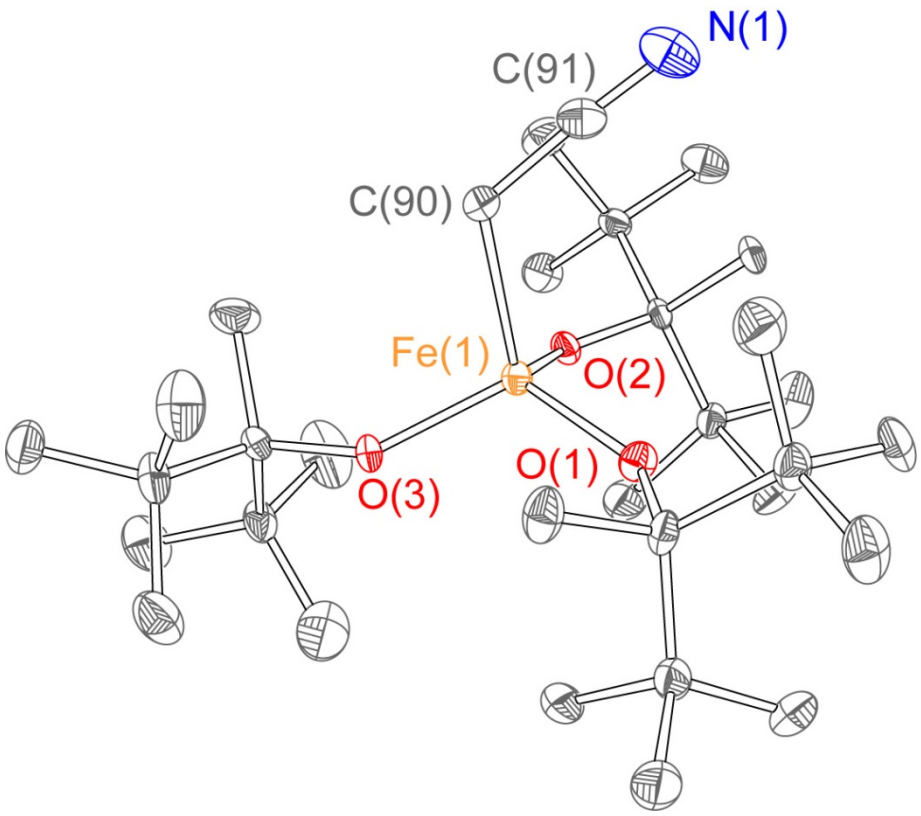


**Figure S5.** Structure $[Fe(ditox)_3(CH_2CN)][K(15C5)_2]$ (**10**), 50% probability ellipsoids. H atoms and $K(15C5)_2$ are omitted for clarity. Selected bond distances: d(Fe1–O1) = 1.859(2) Å, d(Fe1–O2) = 1.845(2) Å, d(Fe1–O3) = 1.846(2) Å, d(Fe1–C90) = 2.141(3) Å, d(C90–C91) = 1.406(5) Å, d(C91–N1) = 1.163(4) Å. Selected bond angles: ∠(O1–Fe1–O2) = 111.6(1)°, ∠(O1–Fe1–O3) = 114.6(1)°, ∠(O2–Fe1–O3) = 110.0(1)°, ∠(O1–Fe1–C90) = 107.9(1)°, ∠(O2–Fe1–C90) = 107.9(1)°, ∠(O3–Fe1–C90) = 104.4(1)°, ∠(C90–C91–N1) = 176.6(4)°.

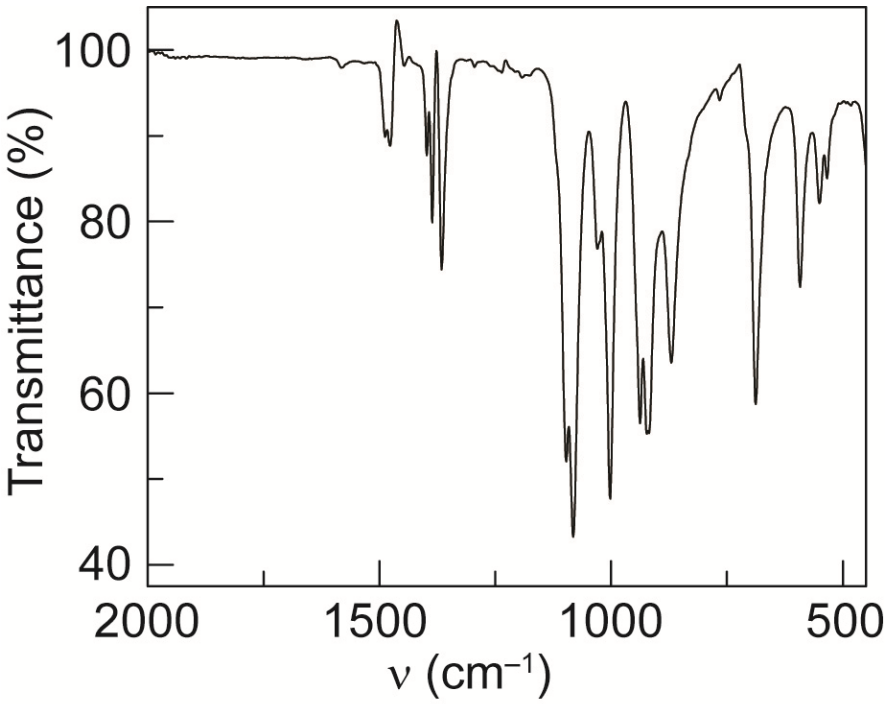


**Figure S6.** IR spectrum of $Fe(ditox)_3(THF)$ (**1**).

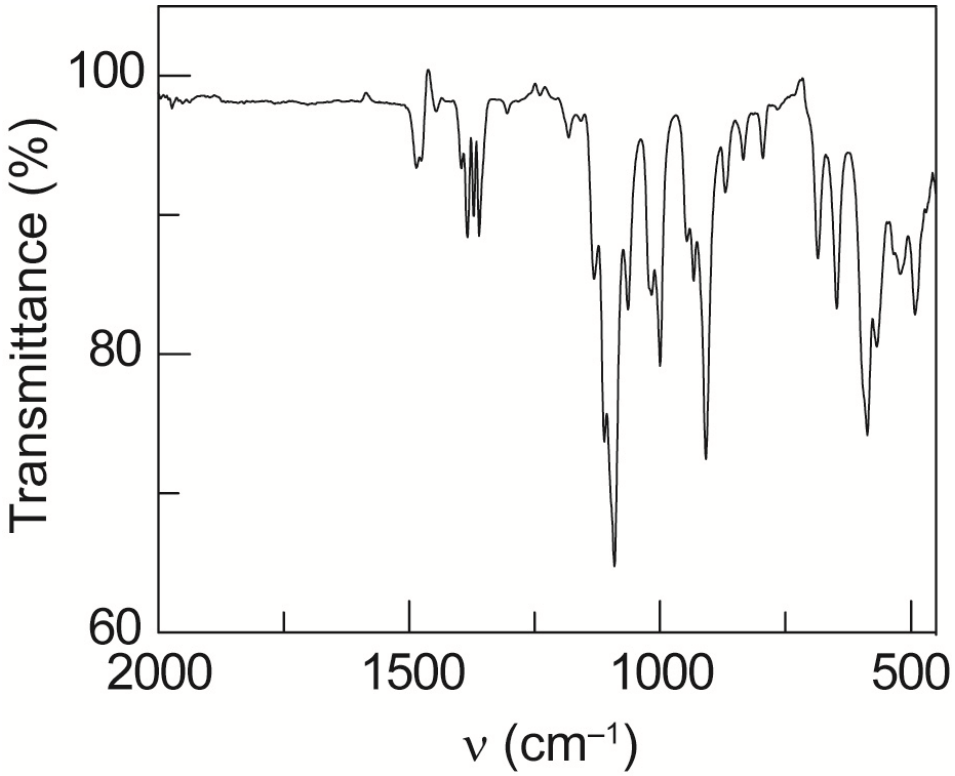


**Figure S7.** IR spectrum of $Fe(ditox)_3Li(OEt_2)$ (**2**).

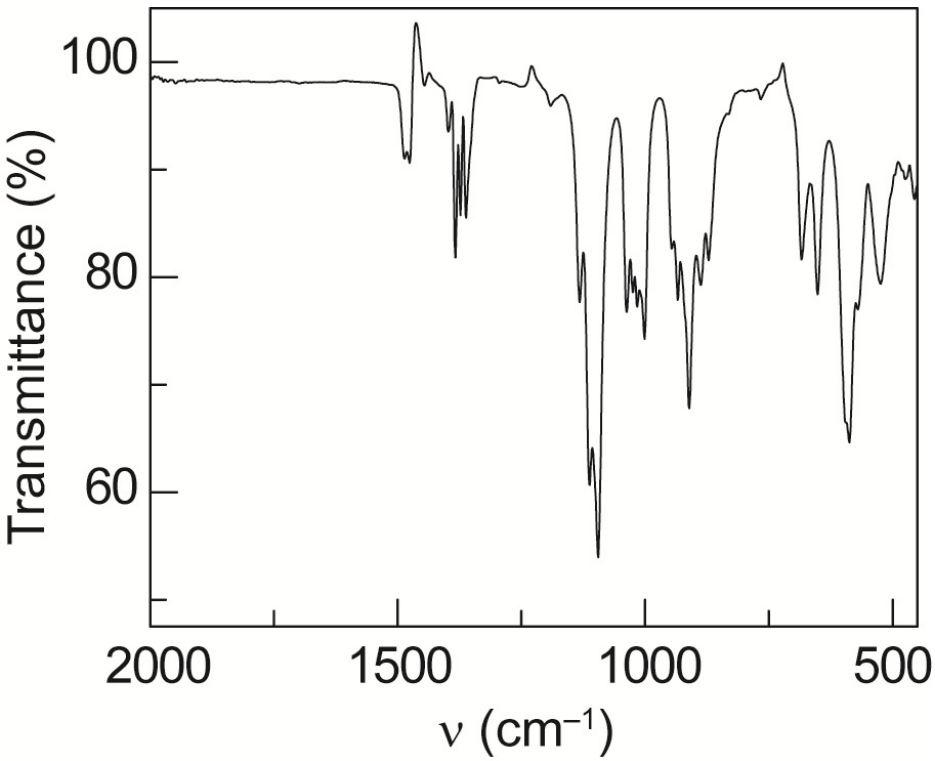


**Figure S8.** IR spectrum of $Fe(ditox)_3Li(THF)$ (**3**).

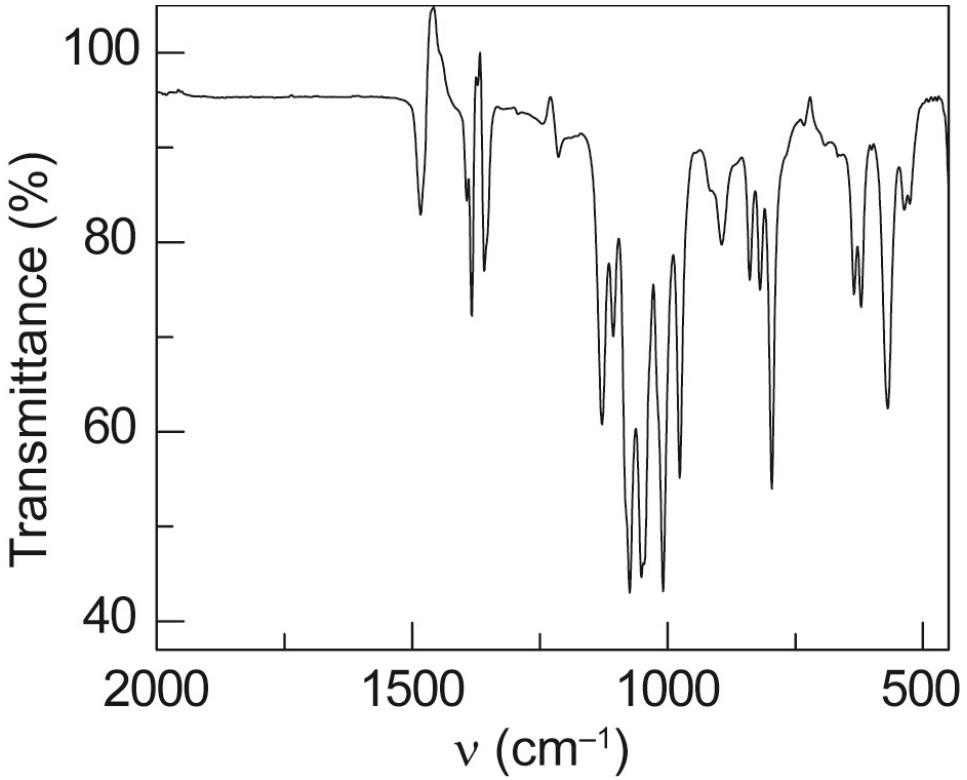


**Figure S9.** IR of $Fe(ditox)_3K(THF)_2$ (**4**).

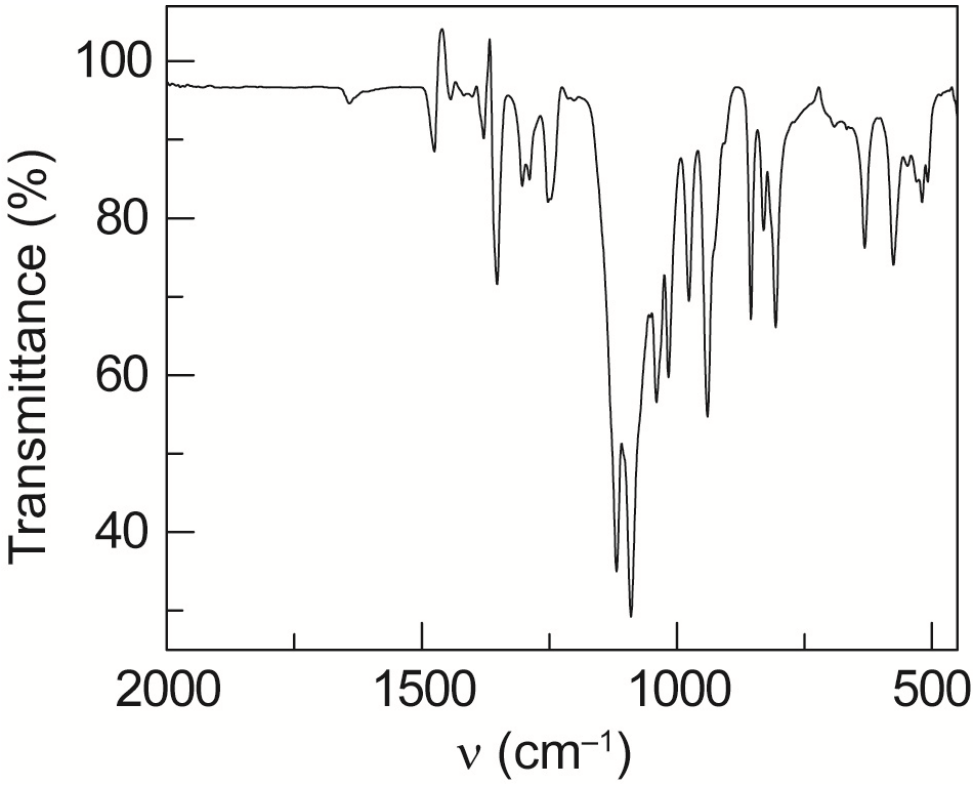


**Figure S10.** $Fe(ditox)_3K(15C5)_2$ (**5**).

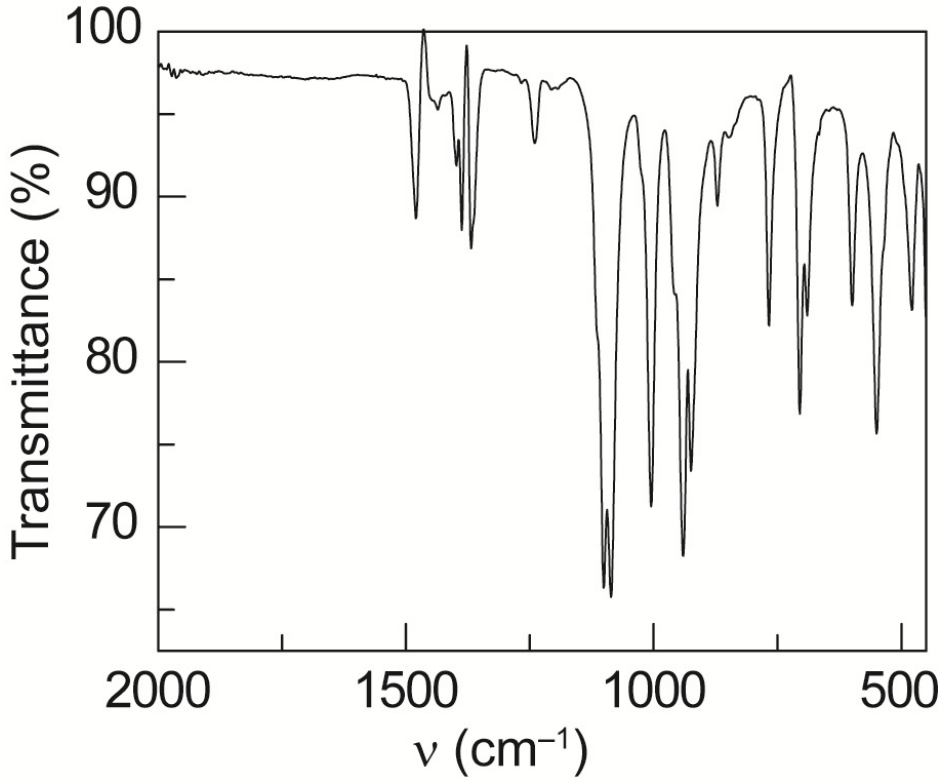


**Figure S11**. IR spectrum of $Fe(ditox)_3(ONMe_3)$ (**6**).

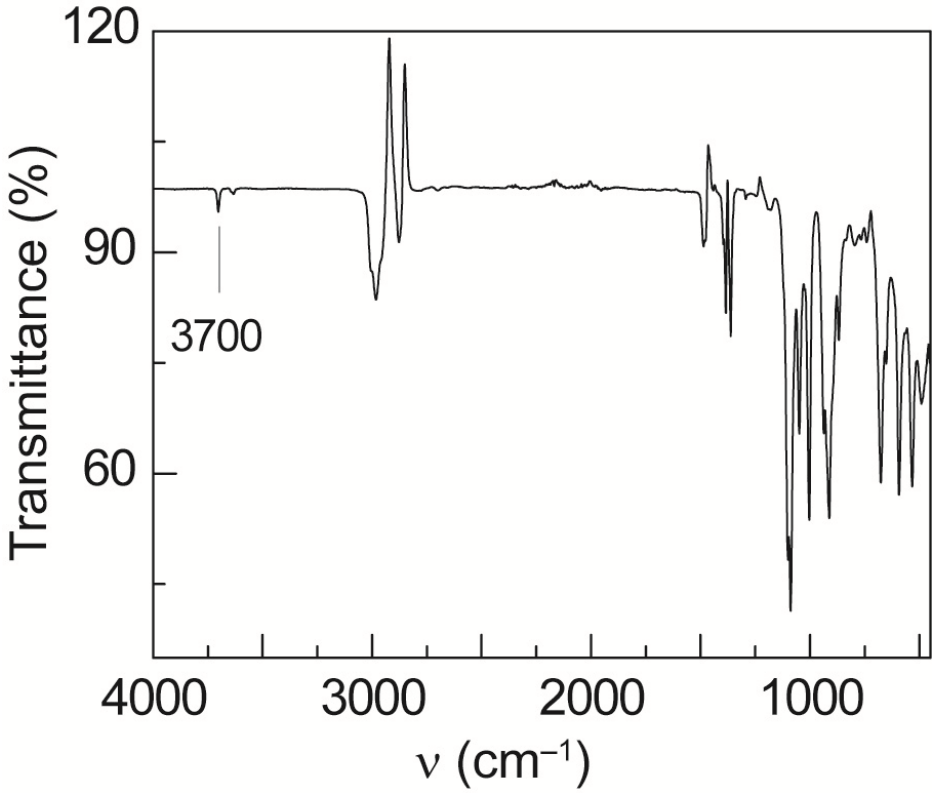


**Figure S12.** IR Spectrum of $Fe(ditox)_3(OH)LiTHF_n$ (**7**/**7a**).

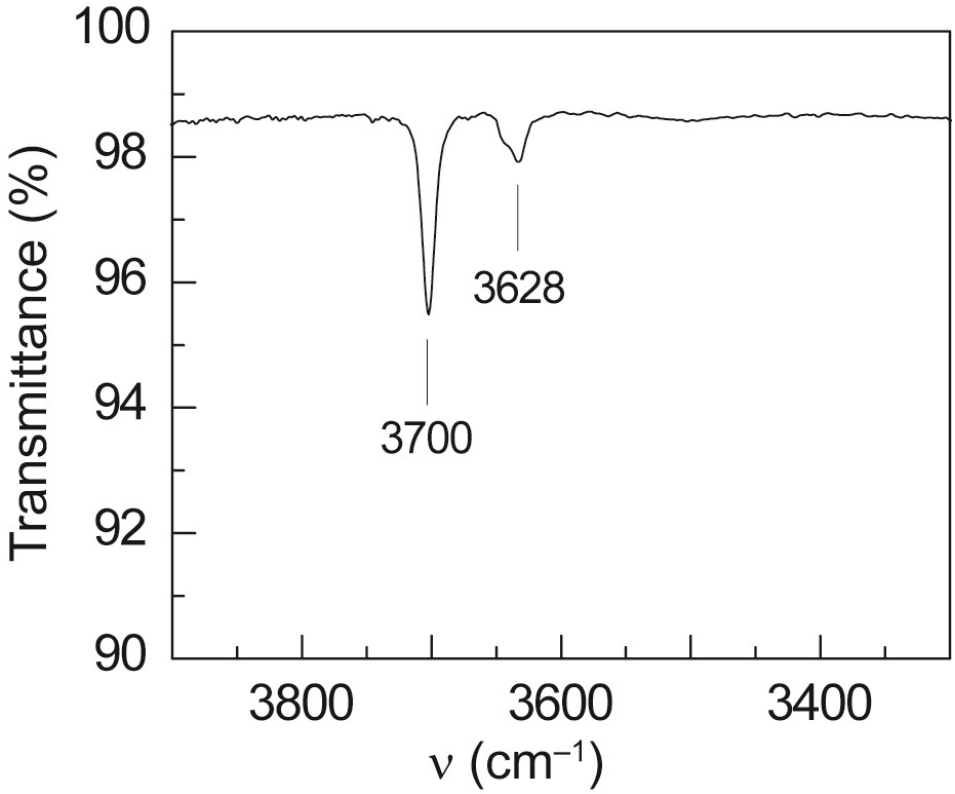


**Figure S13.** IR of $Fe(ditox)_3(OH)Li(THF)_n$ (**7**/**7a**), OH region.

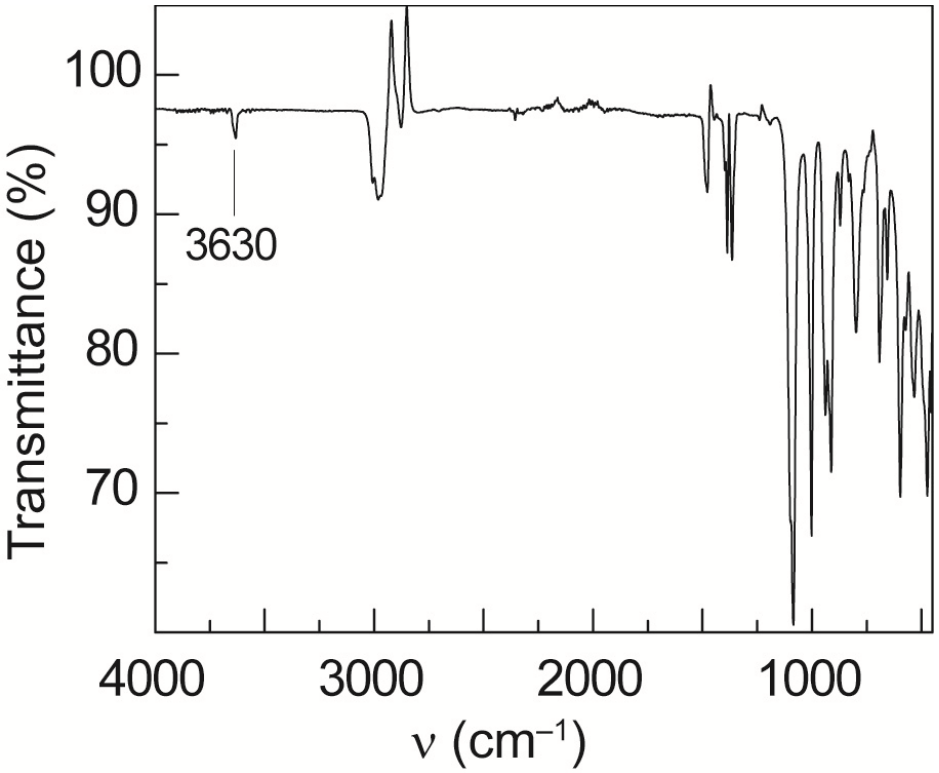


**Figure S14.** IR $Fe(ditox)_3(OH)Li(C_8O_2H_{14})$ (**8**).

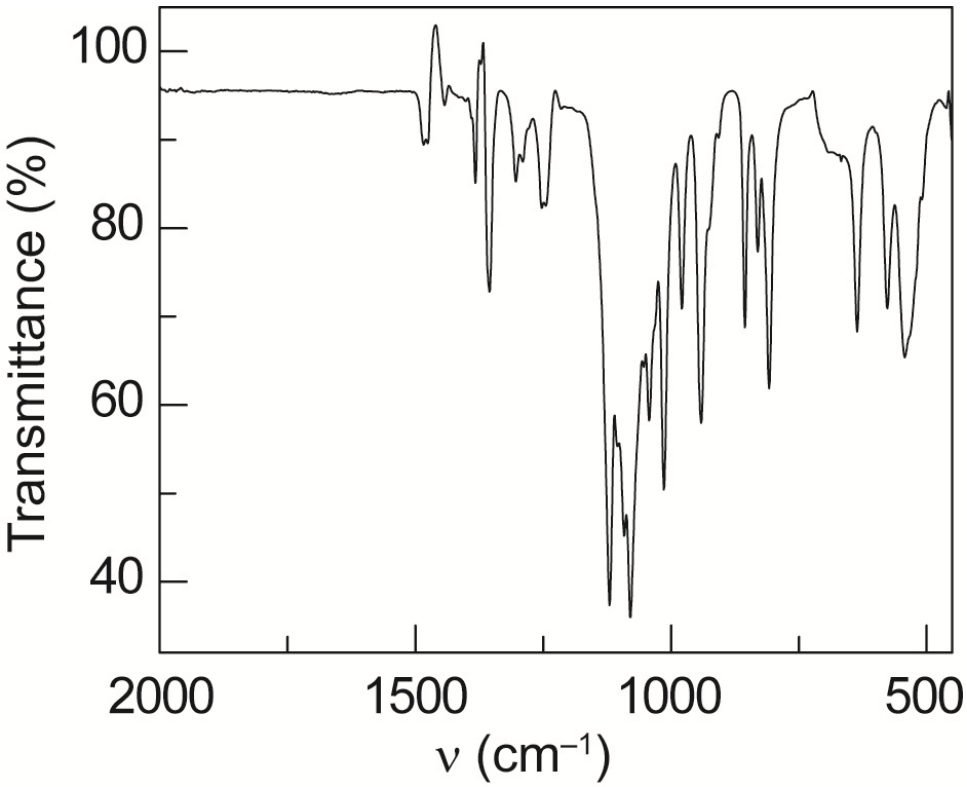


**Figure S15.** $Fe(ditox)_3(OH)K(15C5)_2$ (**9**).

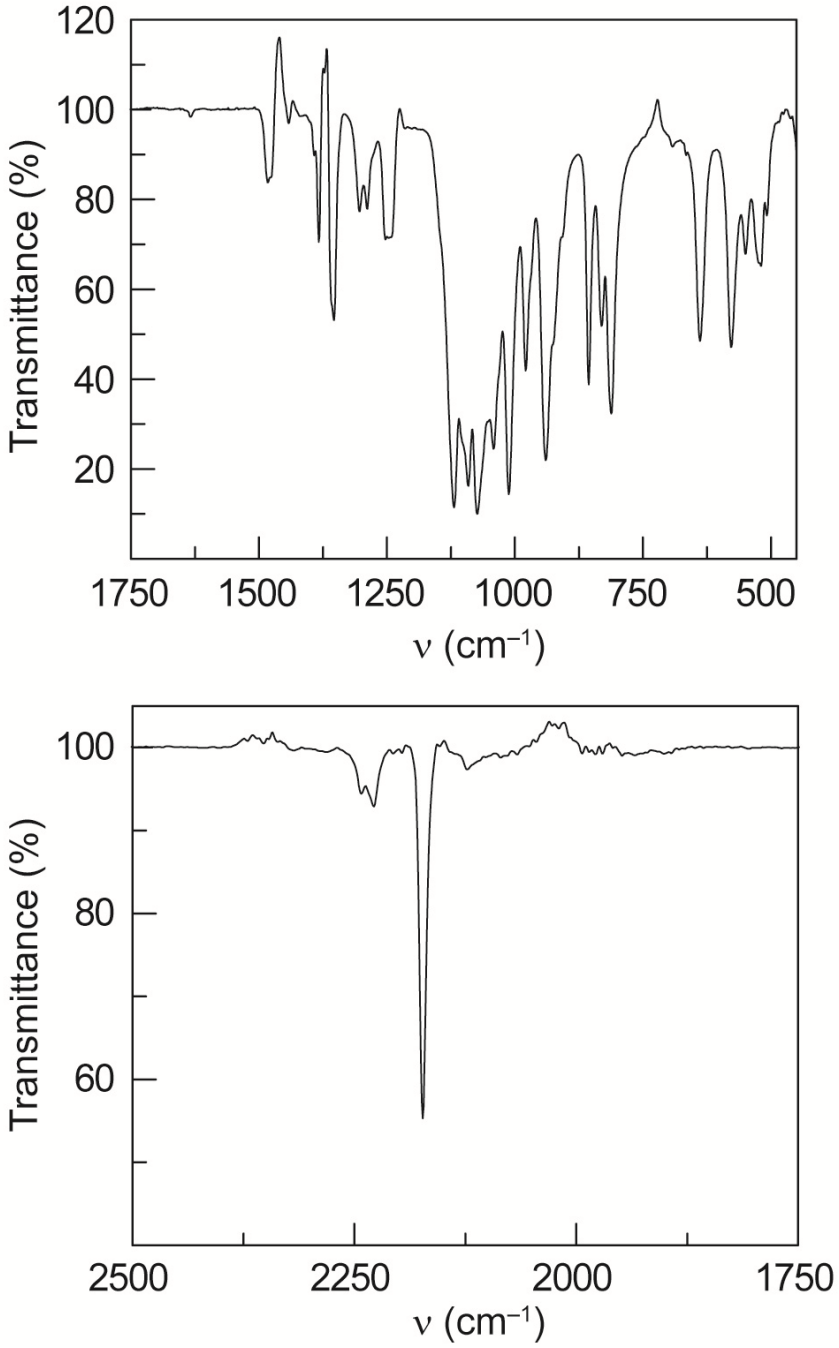


**Figure S16.** IR of $Fe(ditox)_3(CH_2CN)K(15C5)_2$ (**10**).

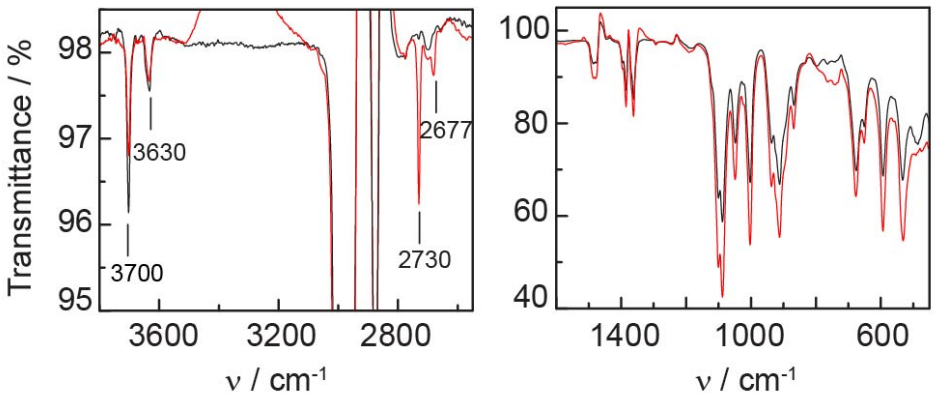


**Figure S17.** IR spectra of **7** prepared in THF (black trace) and THF-$d^8$(red trace). O-H(D) region presented to the left, C–C, C–O and Fe–O region presented to the right

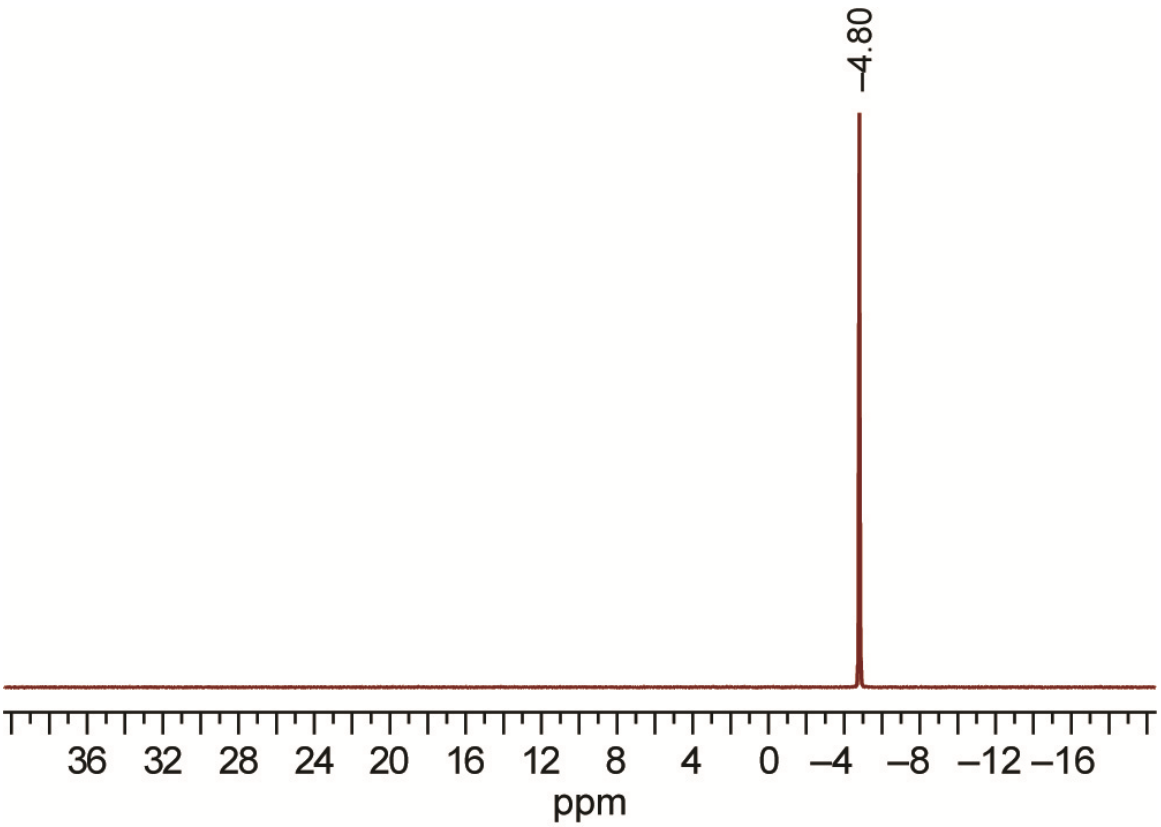


**Figure S18.** $^{31}P$ NMR in $Et_2O$ for reaction of $PPh_3$ with $ONMe_3$ in $C_6H_4F_2$ at room temperature for 1 min. Spectrum referenced to $PPh_3$ at –4.8 ppm. No $OPPh_3$ formation observed.

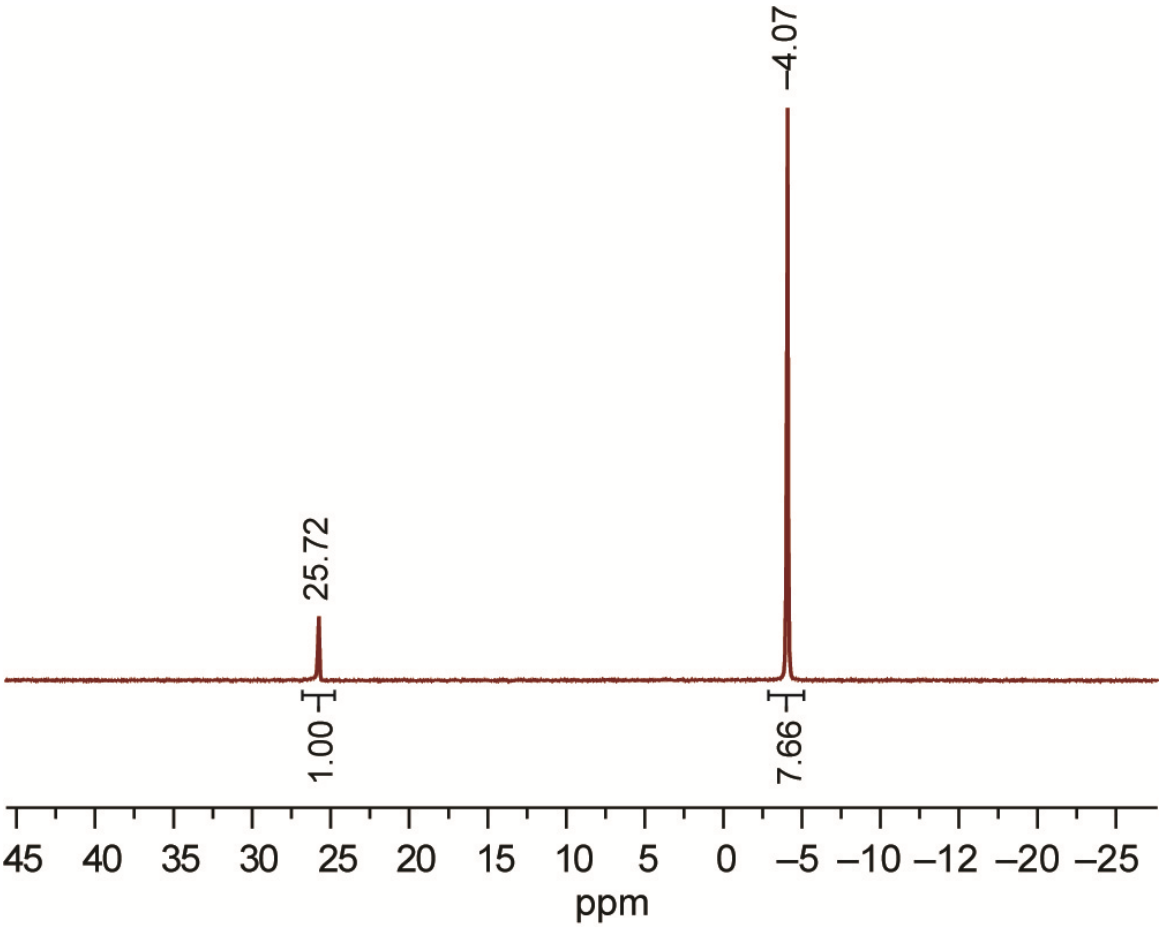


**Figure S19.** $^{31}P$ NMR in $Et_2O$ for reaction of 7 eq $PPh_3$ with 1 eq $ONMe_3$ and 1 eq of $Fe(ditox)_3K(THF)_2$ in $C_6H_4F_2$ at room temperature for 1 min. Spectrum referenced to $PPh_3$ at –4.8 ppm. $OPPh_3$ formation observed at 24.99 ppm. Approximately 77% conversion to $OPPh_3$ observed (vs. $ONMe_3$)

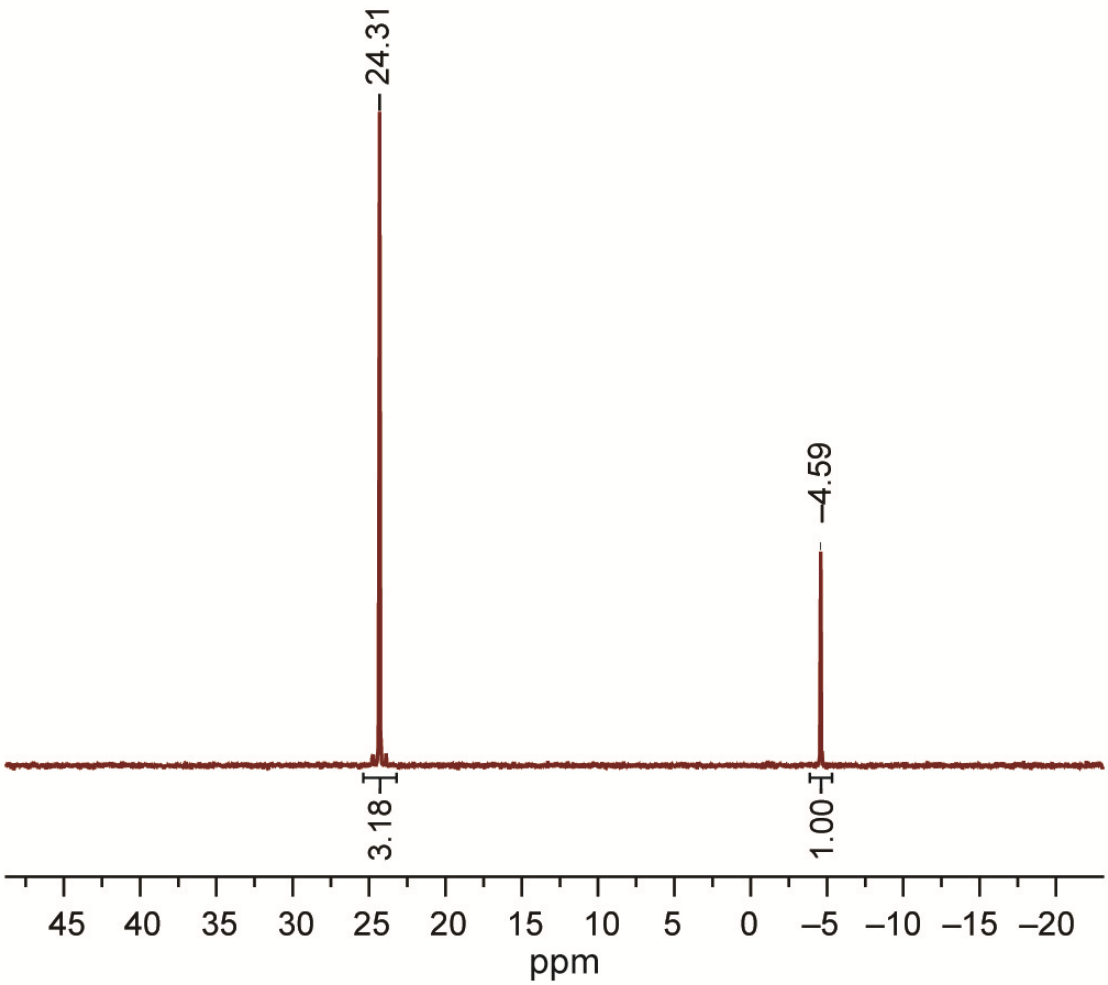


**Figure S20.** $^{31}P$ NMR in $Et_2O$ for reaction of 10 eq $PPh_3$ with 10 eq $ONMe_3$ and 1 eq of $Fe(ditox)_3K(THF)_2$ in $C_6H_4F_2$ at room temperature for 1 min. Spectrum referenced to $PPh_3$ at –4.8 ppm. $OPPh_3$ formation observed at 24.10 ppm representing 7.6 turnovers of $Fe(ditox)_3(THF)_2$.

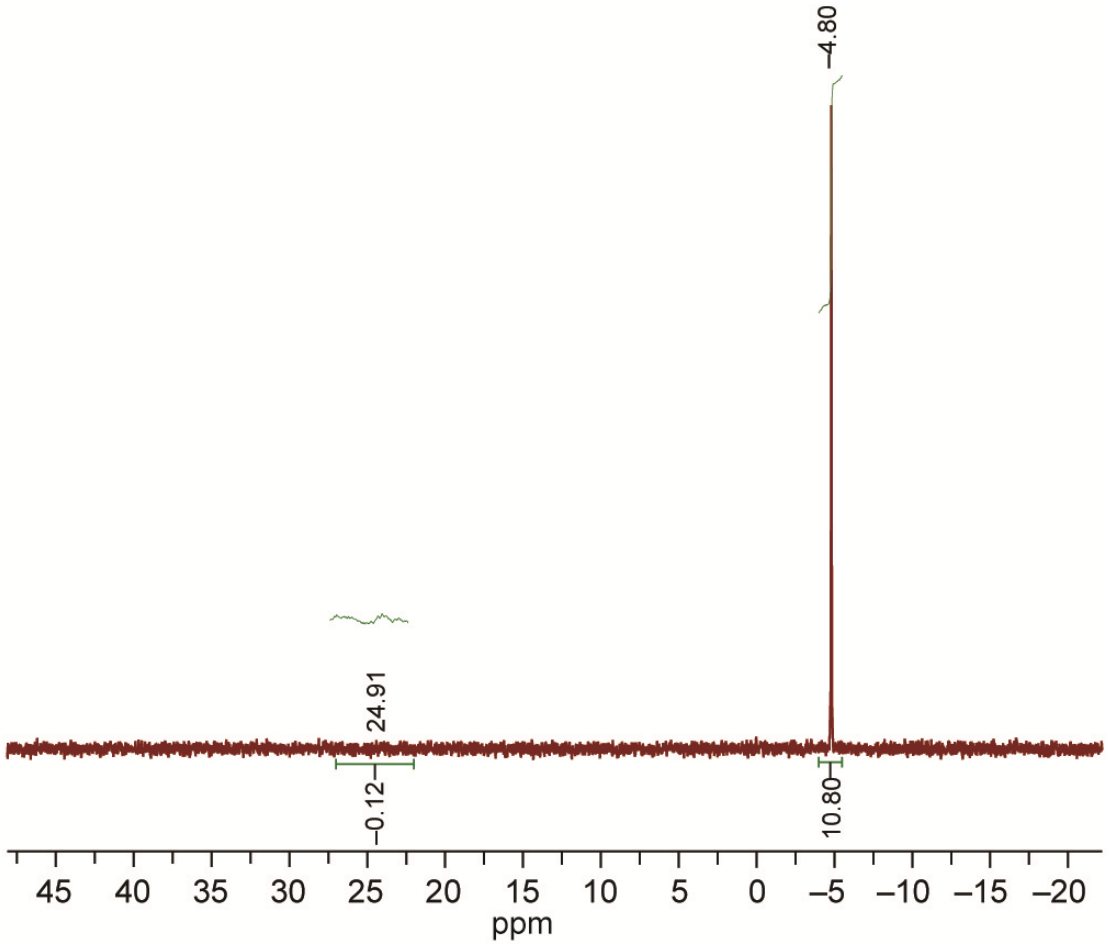


**Figure S21.** $^{31}P$ NMR in $Et_2O$ for reaction of 1 eq $PPh_3$ with 1 eq $ONMe_3$ in THF at room temperature for 1 min. Spectrum referenced to $PPh_3$ at –4.8 ppm. No $OPPh_3$ formation observed as no discernible peak is seen in the expected region of $OPPh_3$ and no appreciable signal integration is found.

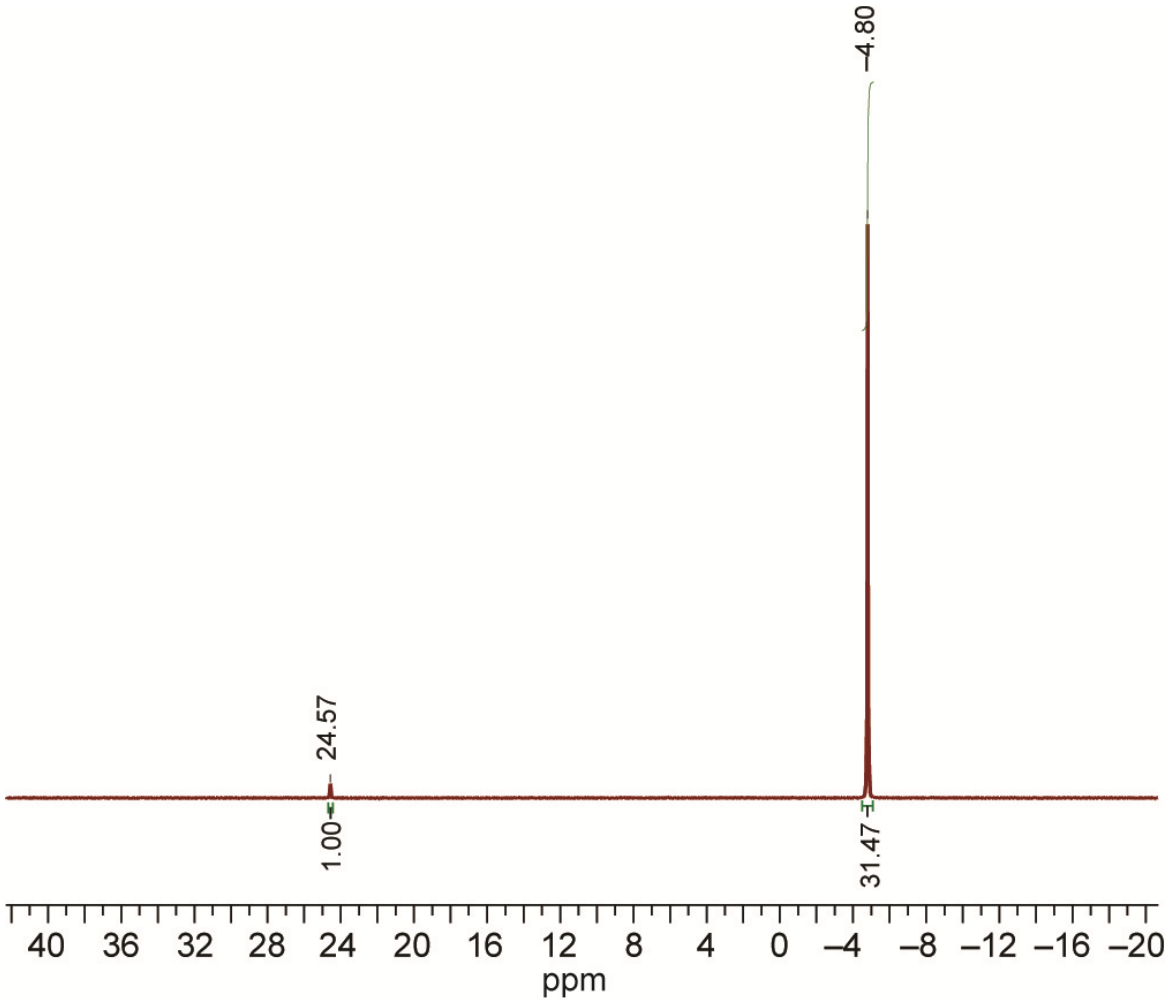


**Figure S22.** $^{31}P$ NMR in $Et_2O$ for reaction of 10 eq $PPh_3$ with 1 eq $ONMe_3$ and 1 eq of $Fe(ditox)_3K(THF)_2$ in THF at room temperature for 1 min. Spectrum referenced to $PPh_3$ at –4.8 ppm. $OPPh_3$ formation observed at 24.63 ppm with 20% of $PPh_3$ converted to $OPPh_3$ (yield based on moles of $ONMe_3$).

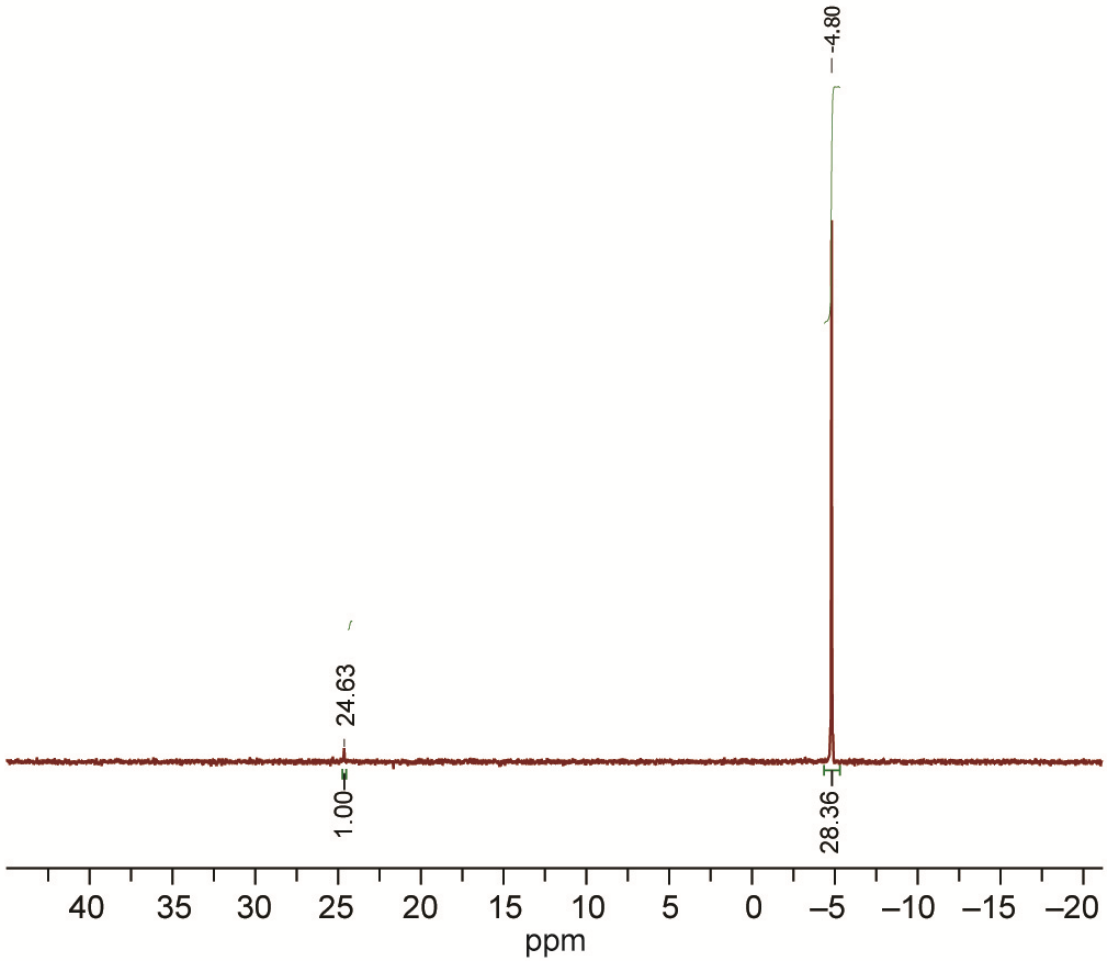


**Figure S23.** $^{31}P$ NMR in $Et_2O$ for reaction of 10 eq $PPh_3$ with 10 eq $ONMe_3$ and 1 eq of $Fe(ditox)_3K(THF)_2$ in THF at room temperature for 1 minute. Spectrum referenced to $PPh_3$ at –4.8 ppm. $OPPh_3$ formation observed at 24.37 ppm with 3.4% of $PPh_3$ converted to $OPPh_3$ (yield based on moles of $ONMe_3$).

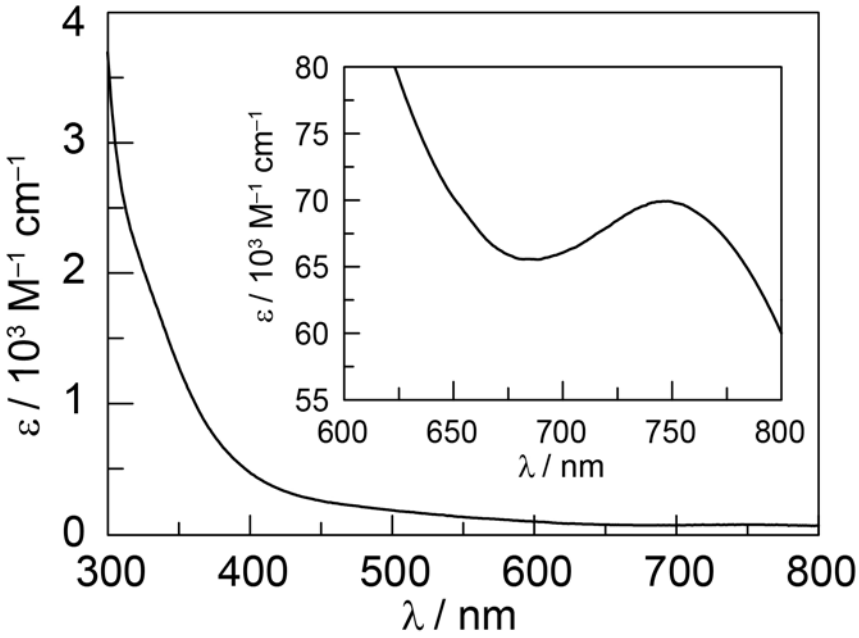


**Figure S24**. UV-vis spectrum of $Fe(ditox)_3Li(Et_2O)_2$ in a THF solution. (Inset) Expanded spectrum shows weak absorption maximum at 748 nm.

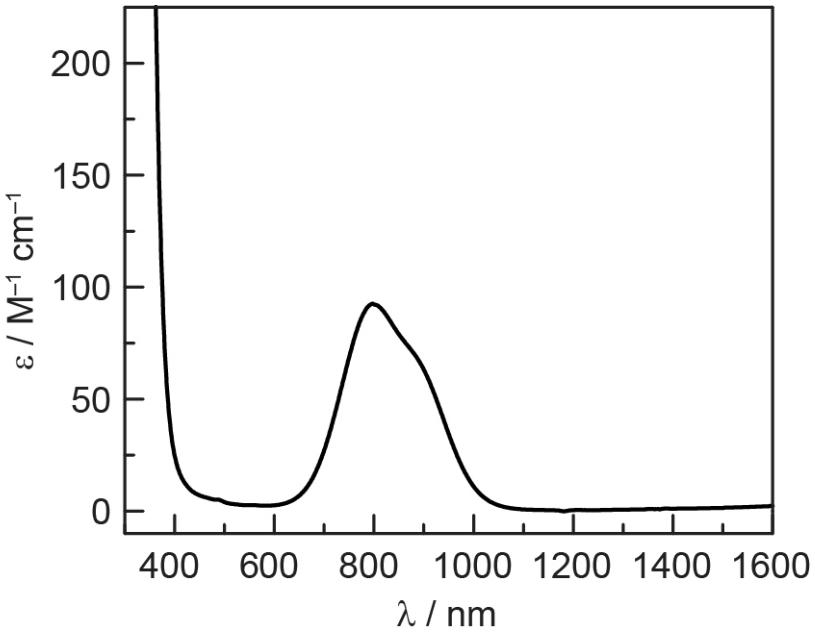


**Figure S25**. UV-vis spectrum of $[Fe(Ditox)_3][K(15C5)_2]$ in a THF solution between 300 nm and 1600 nm with an absorption maximum 798 nm.

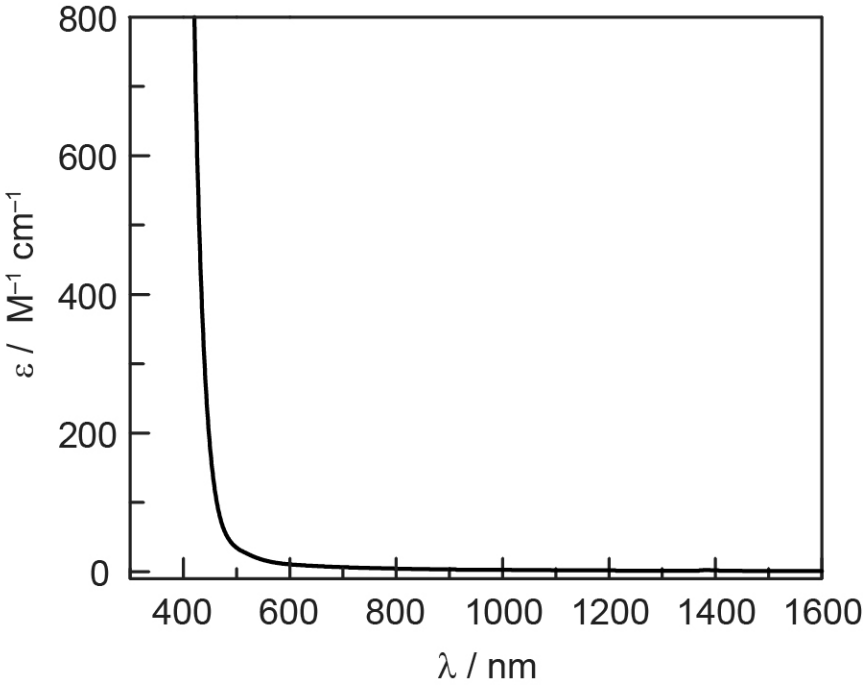


**Figure S26**. UV-vis spectrum of Fe(ditox)$_3$THF in a THF; there is no discernible absorption maximum in the spectrum.

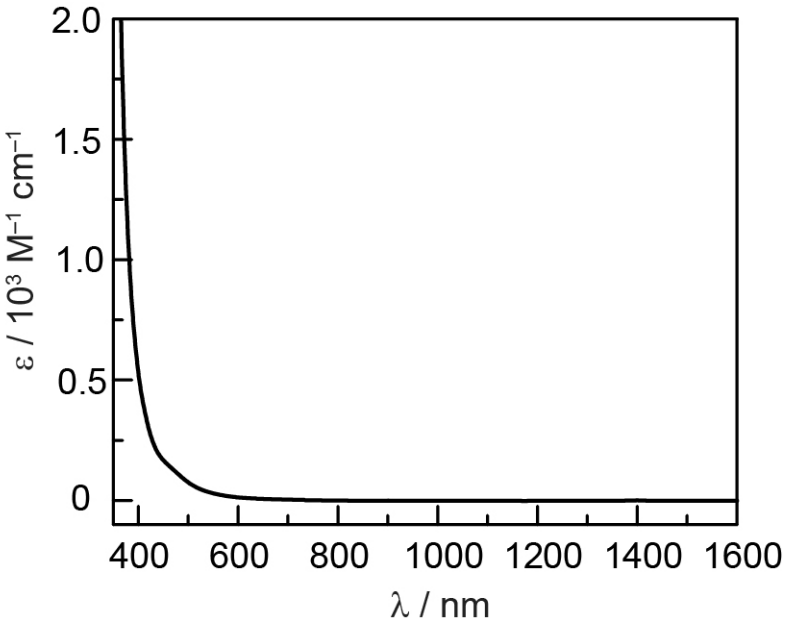


**Figure S27**. UV-vis spectrum of $[Fe(ditox)_3(OH)][K(15C5)_2]$ in a THF.

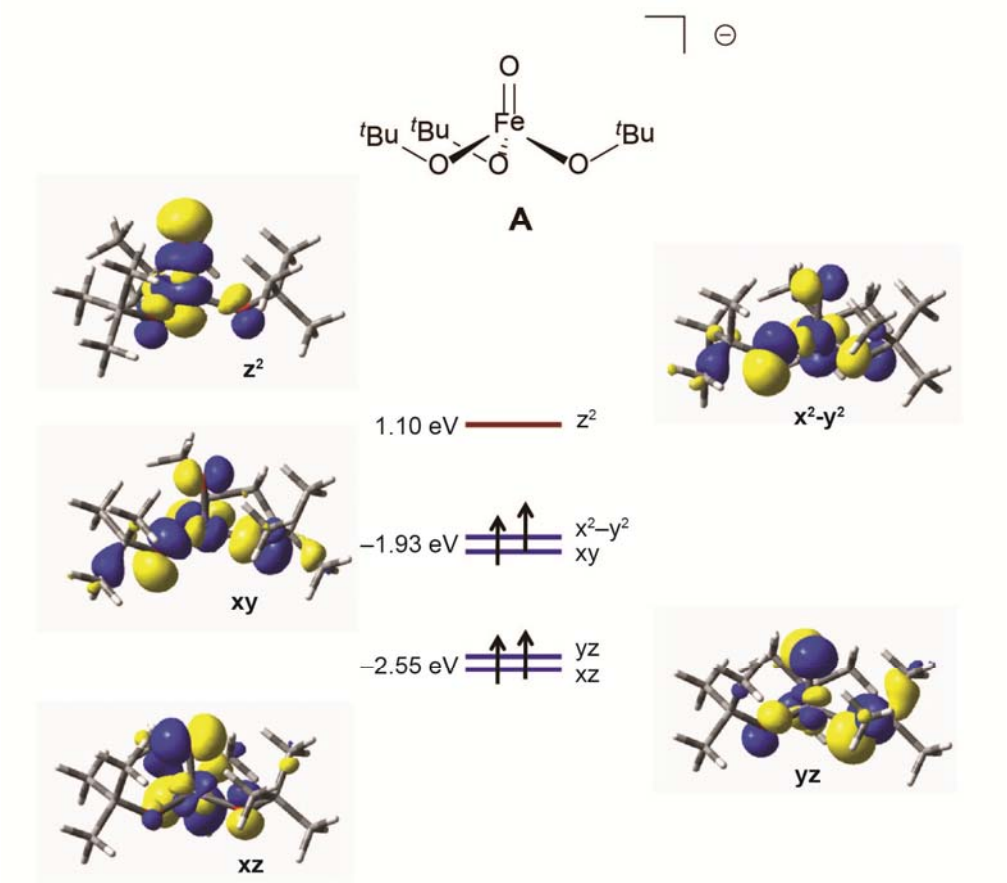


**Figure S28.** Calculated molecular orbital diagram for $[Fe(O^tBu)_3(O)]^-$. Molecular orbitals shown depicted for alpha spins with an isovalue of 0.4.

**Table S2.** Calculated atomic orbital composition of frontier molecule orbitals for $[Fe(OtBu)_3(O)]^-$.

| Orbital | | O (oxo) | Fe | O (alkoxide) |
|---|---|---|---|---|
| LUMO | $z^2$ | 30% | 44% | 17% |
| SOMO | $x^2–y^2$ | 7% | 22% | 46% |
| SOMO–1 | xy | 7% | 21% | 47% |
| SOMO–2 | yz | 19% | 12% | 38% |
| SOMO–3 | xz | 24% | 13% | 36% |

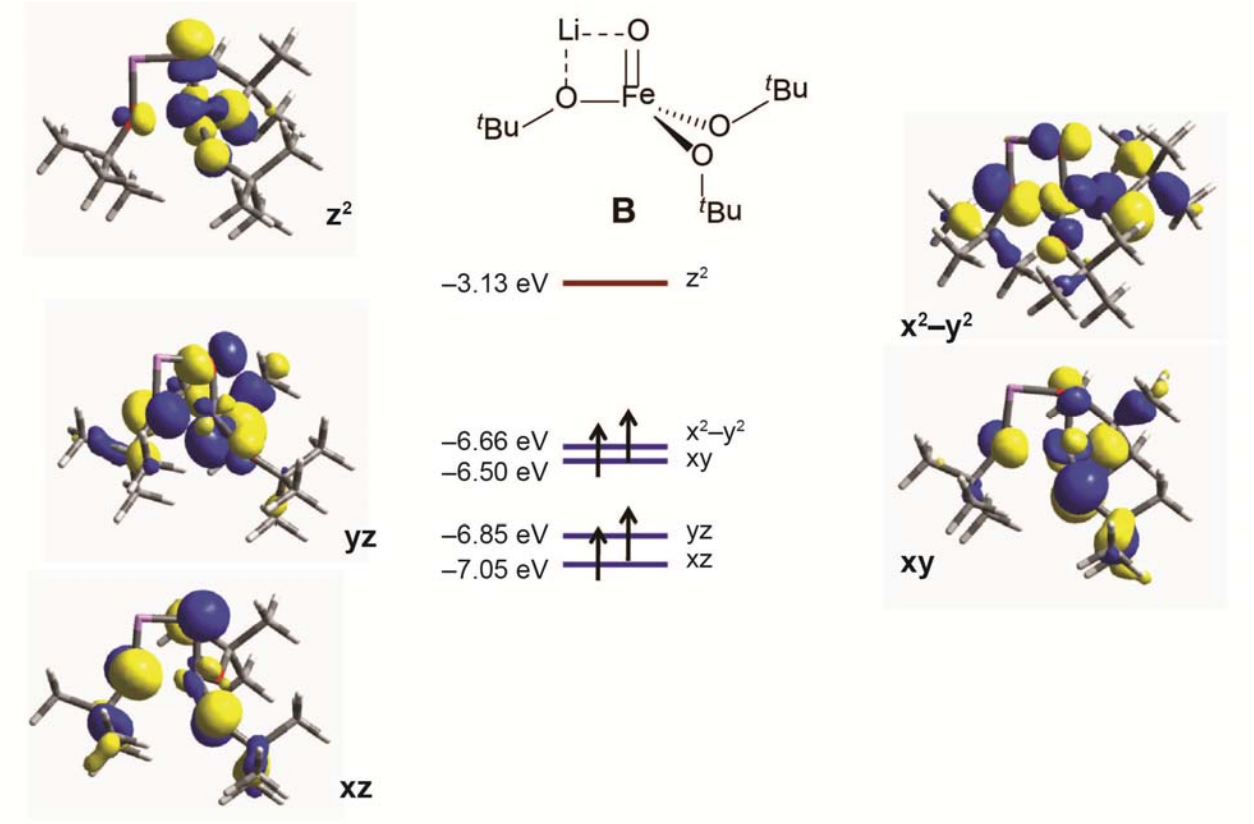


**Figure S29.** Calculated molecular orbital diagram for Fe(O$^t$Bu)$_3$(O)Li. Molecular orbitals shown depicted for alpha spins with an isovalue of 0.4.

**Table S3.** Calculated atomic orbital composition of frontier molecule orbitals for Fe(OtBu)3(O)Li.

| Orbital | | O (oxo) | Fe | O (alkoxide) | Li |
|---|---|---|---|---|---|
| LUMO | $z^2$ | 20% | 42% | 26% | 1% |
| SOMO | $x^2–y^2$ | 13% | 22% | 40% | 1% |
| SOMO–1 | xy | 7% | 19% | 47% | 2% |
| SOMO–2 | yz | 5% | 13% | 49% | 1% |
| SOMO–3 | xz | 27% | 7% | 41% | 1% |

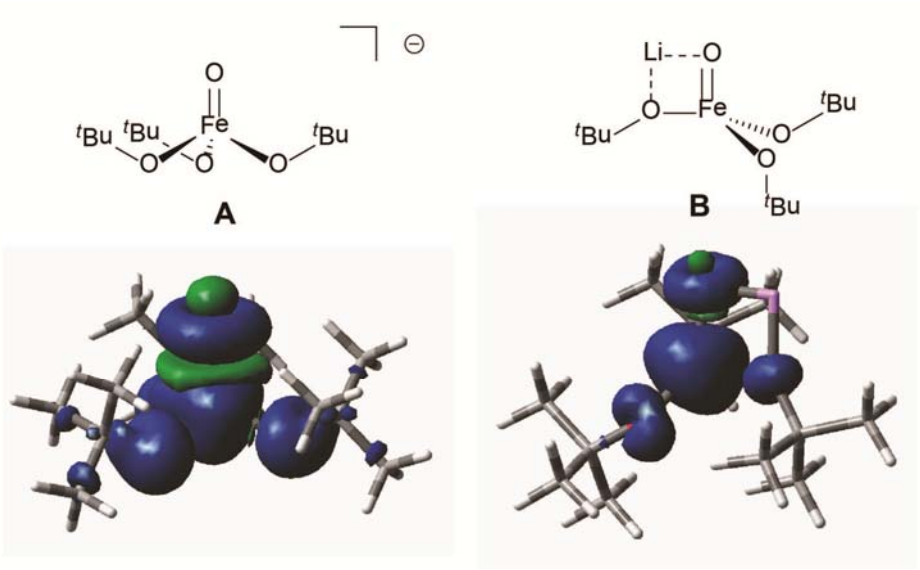


**Figure S30.** Calculated residual spin density contour maps for $[Fe(O^tBu)_3(O)]^-$ (left) and $Fe(O^tBu)_3(O)Li$ (right). Oxo atom spin density character for $[Fe(O^tBu)_3(O)]^-$ and $Fe(O^tBu)_3(O)Li$ is 14% and 13%, respectively.

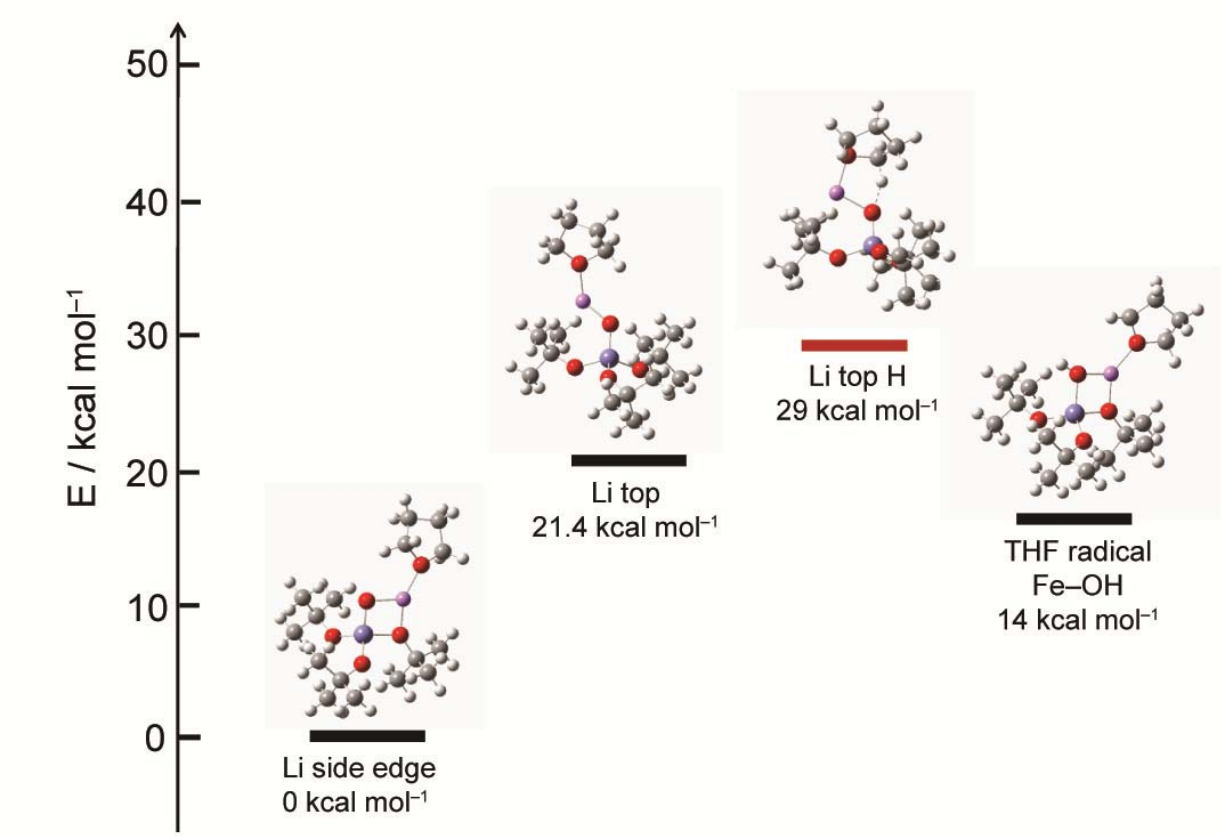


**Figure S31.** Energy diagram of calculated reaction profiled for H–atom abstraction form THF by $Fe(O^tBu)_3(O)Li$.

**Table S5.** Cartesian coordinates for the DFT optimized geometry for the S = 2 model of $[Fe(O^tBu)_3(O)]^-$ (E = –897.902974289 hartrees).

| | *x* | *y* | *z* |
|---|---|---|---|
| Fe | 0.04100300 | –0.02635100 | –0.11964000 |
| O | 1.79138600 | –0.14121900 | –0.73783000 |
| O | –0.86947100 | –1.57301300 | –0.64334000 |
| C | –1.08578500 | 2.76685700 | –0.09430500 |
| C | 3.01514500 | –0.49251600 | –0.10279700 |
| C | –1.96856100 | –2.27645600 | –0.08832100 |
| O | –0.84732700 | 1.50099000 | –0.70017100 |
| O | 0.10841700 | 0.06229100 | 1.51312300 |
| C | –1.54776600 | –2.91970400 | 1.25951900 |
| H | –2.38297800 | –3.45710200 | 1.73577700 |
| H | –0.72207100 | –3.62413000 | 1.09096100 |
| H | –1.18904900 | –2.13245300 | 1.93367000 |
| C | –2.36145600 | –3.37988600 | –1.10645500 |
| H | –1.49472100 | –4.02660400 | –1.29577100 |
| H | –3.19660600 | –3.99775400 | –0.74077400 |
| H | –2.65153100 | –2.91579100 | –2.05852700 |
| C | –3.16952100 | –1.31887700 | 0.13490200 |
| H | –2.89257000 | –0.54376400 | 0.85910100 |
| H | –3.42323000 | –0.82118700 | –0.81000100 |
| H | –4.05484200 | –1.85701600 | 0.50901700 |
| C | 2.87751000 | –1.86466100 | 0.61010100 |
| H | 2.09141900 | –1.79955900 | 1.37133500 |
| H | 2.58179300 | –2.63073600 | –0.11892300 |
| H | 3.82101100 | –2.17006200 | 1.08997300 |
| C | 4.08707700 | –0.58266900 | –1.21971200 |
| H | 4.16015000 | 0.38259300 | –1.73798900 |
| H | 5.07646100 | –0.84774600 | –0.81550800 |
| H | 3.78620100 | –1.34081000 | –1.95457100 |
| C | 3.40514600 | 0.60120100 | 0.92628600 |
| H | 4.35290900 | 0.36563500 | 1.43582100 |
| H | 3.50686300 | 1.56895000 | 0.41649400 |
| H | 2.60481600 | 0.68811600 | 1.67032100 |
| C | –2.10446400 | 2.61097800 | 1.06584000 |
| H | –3.05290900 | 2.21630800 | 0.67652900 |
| H | –1.70515300 | 1.89602800 | 1.79459100 |

| | | | |
|---|---|---|---|
| H | –2.29875600 | 3.57111800 | 1.56884700 |
| C | –1.67240600 | 3.68238500 | –1.20049000 |
| H | –1.92175900 | 4.68247400 | –0.81238100 |
| H | –0.94519800 | 3.78770700 | –2.01637800 |
| H | –2.58047800 | 3.22313000 | –1.61262200 |
| C | 0.24004600 | 3.36759000 | 0.44319400 |
| H | 0.96532900 | 3.44986400 | –0.37671200 |
| H | 0.08594100 | 4.36403900 | 0.88671400 |
| H | 0.65904300 | 2.69601200 | 1.20082800 |

**Table S6.** Cartesian coordinates for the DFT optimized geometry for the S = 1 model of $[Fe(O^tBu)_3(O)]^-$ (E = –897.879633387 hartrees).

| | *x* | *y* | *z* |
|---|---|---|---|
| Fe | –0.02499800 | –0.32061300 | –0.39803700 |
| O | –1.57846600 | –0.39451600 | 0.61367100 |
| O | 1.37065100 | –1.43387100 | 0.00177900 |
| C | 0.16569200 | 2.51168900 | 0.12995100 |
| C | –2.81100300 | –1.03820600 | 0.27505100 |
| C | 2.76821400 | –1.22554600 | 0.20309300 |
| O | 0.83010600 | 1.24004300 | 0.03667900 |
| O | –0.53088700 | –0.40476300 | –1.92920800 |
| C | 3.36825300 | –0.40096200 | –0.96398700 |
| H | 4.45663100 | –0.27480400 | –0.85054700 |
| H | 3.16592900 | –0.91122800 | –1.91534200 |
| H | 2.88586400 | 0.58102500 | –0.99205900 |
| C | 3.40504000 | –2.64104900 | 0.22843300 |
| H | 3.20960600 | –3.14965800 | –0.72487700 |
| H | 4.49284800 | –2.59373300 | 0.39289700 |
| H | 2.94864800 | –3.23596300 | 1.03074400 |
| C | 3.01536200 | –0.51318700 | 1.55799000 |
| H | 2.50462400 | 0.45453300 | 1.54483500 |
| H | 2.59462000 | –1.11749100 | 2.37382900 |
| H | 4.09027600 | –0.36264500 | 1.74640700 |
| C | –2.55808400 | –2.47354400 | –0.25586100 |
| H | –1.97441100 | –2.42175300 | –1.18230000 |
| H | –1.97949800 | –3.04397800 | 0.48318900 |
| H | –3.50312300 | –3.00325800 | –0.45437100 |
| C | –3.63000300 | –1.10522000 | 1.59075000 |
| H | –3.78035900 | –0.09151400 | 1.98492000 |
| H | –4.61304200 | –1.57505100 | 1.43255900 |
| H | –3.07513900 | –1.68273700 | 2.34176700 |
| C | –3.57268700 | –0.20734200 | –0.78840000 |
| H | –4.51760300 | –0.69172900 | –1.08032300 |
| H | –3.79875200 | 0.79230500 | –0.39152000 |
| H | –2.93104200 | –0.09731600 | –1.66987100 |
| C | –0.73279300 | 2.78330300 | –1.10152600 |
| H | –0.14538000 | 2.67748100 | –2.02204300 |
| H | –1.54949000 | 2.05689100 | –1.14630600 |

| | | | |
|---|---|---|---|
| H | –1.15709200 | 3.79854800 | –1.05818800 |
| C | 1.31128000 | 3.55784300 | 0.17209500 |
| H | 0.91773500 | 4.57840300 | 0.29350200 |
| H | 1.98390400 | 3.33485800 | 1.01035400 |
| H | 1.89447600 | 3.50949200 | –0.75689300 |
| C | –0.66518800 | 2.58273500 | 1.43586700 |
| H | –0.00431700 | 2.45506100 | 2.30466800 |
| H | –1.18813600 | 3.54752500 | 1.52940200 |
| H | –1.39356600 | 1.76444100 | 1.44043800 |

**Table S7.** Cartesian coordinates for the DFT optimized geometry for the S=0 model of $[Fe(O^tBu)_3(O)]^-$ (E = –897.880371127 hartrees).

| | *x* | *y* | *z* |
|---|---|---|---|
| Fe | 0.00134700 | –0.00085700 | –0.69516100 |
| O | 1.43594200 | –0.81259700 | 0.06050600 |
| O | –0.01294800 | 1.64813100 | 0.06234000 |
| C | –1.48599400 | –2.25358800 | 0.27639500 |
| C | 2.69750300 | –0.15815300 | 0.27617200 |
| C | –1.21143400 | 2.41269200 | 0.27643400 |
| O | –1.41719500 | –0.83192100 | 0.07011600 |
| O | –0.00279200 | –0.00098700 | –2.28365400 |
| C | –2.23505800 | 2.22335100 | –0.87157600 |
| H | –3.10431100 | 2.88491800 | –0.73349100 |
| H | –1.76049300 | 2.44738700 | –1.83491600 |
| H | –2.57719800 | 1.18257600 | –0.89587800 |
| C | –0.74928600 | 3.89150300 | 0.33008000 |
| H | –0.30986500 | 4.17636800 | –0.63504100 |
| H | –1.58707700 | 4.56880500 | 0.55572300 |
| H | 0.02090700 | 4.00911800 | 1.10376300 |
| C | –1.84411000 | 1.99434100 | 1.62858500 |
| H | –2.06726700 | 0.92261500 | 1.59023800 |
| H | –1.13070200 | 2.17242800 | 2.44535400 |
| H | –2.76839500 | 2.55618200 | 1.83748100 |
| C | 3.04574100 | 0.82689300 | –0.86821600 |
| H | 3.00325300 | 0.30788700 | –1.83379900 |
| H | 2.31637900 | 1.64444700 | –0.88908100 |
| H | 4.05352300 | 1.24819700 | –0.72851200 |
| C | 2.65171700 | 0.59395900 | 1.63121000 |
| H | 2.43271600 | –0.11465800 | 2.44196300 |
| H | 3.60524800 | 1.10038600 | 1.85044100 |
| H | 1.84516100 | 1.33410100 | 1.59012500 |
| C | 3.74663000 | –1.29819200 | 0.32616600 |
| H | 4.75225200 | –0.91176300 | 0.55143700 |
| H | 3.46373300 | –2.02531600 | 1.09875400 |
| H | 3.77262700 | –1.81924400 | –0.64004900 |
| C | –0.80697400 | –3.04240100 | –0.87156200 |
| H | –1.23889400 | –2.74614200 | –1.83539400 |
| H | 0.26479200 | –2.81513900 | –0.89535600 |

| | | | |
|---|---|---|---|
| H | –0.94072900 | –4.12675800 | –0.73353100 |
| C | –2.99894600 | –2.58882900 | 0.32156400 |
| H | –3.17014300 | –3.65478800 | 0.53562000 |
| H | –3.48674700 | –1.98720300 | 1.09987400 |
| H | –3.46139800 | –2.33950100 | –0.64258700 |
| C | –0.81574400 | –2.60086000 | 1.63058200 |
| H | –1.32740200 | –2.06930100 | 2.44486700 |
| H | –0.85019400 | –3.68244600 | 1.83655700 |
| H | 0.22687300 | –2.26618900 | 1.60015100 |